Supplementary Material: Mechanism of UV-induced Dewar lesions repair catalyzed by DNA (6-4) Photolyase

Benjamin P. Fingerhut, Korbinian Heil, Emine Kaya, Sven Oesterling, Regina de Vivie-Riedle and Thomas Carell.*

Center for Integrated Protein Science Munich (CIPSM), Department of Chemistry, Ludwig-Maximilians University Munich, Butenandtstr. 5-13, 81377 Munich, Germany, Fax: +49 (0)89 2180 77756; Tel: +49 (0)89 2180 77750; E-mail: Thomas.Carell@cup.uni-muenchen.

Theoretical Methods:

Activation energies ΔE_A of radical-anionic Dewar photolesion repair:

The geometries of four different Dewar-photolesion (T(dew)C, T(dew)U, T(dew)^{m}C, T(dew)T) have been optimized with the hybrid meta-GGA functional M05-2X.[1] This functional shows the best reported performance for electron affinities and dissociation energies[2] (radical anionic repair mechanism and N3-C6 bond cleavage!). In all calculations aqueous surrounding is considered by an electrostatic continuum model (SCRF = PCM, H_2O; ε=78.4)[3] as implemented in the Gaussian09 programm package,[4] using a 6-31G* double zeta basis set. The impact of the basis size on the calculated reaction barriers were tested using the larger basis sets 6-31+G* and 6-31+G** for the T(dew)C lesion. The impact of solvent polarity was tested choosing an unpolar dibutylether (ε=3) as second solvent. Additional calculations on all four Dewar-photolesion have been performed with the M06-2X functional [2] and the popular hybrid

exchange correlation B3LYP functional,[5] for T(dew)C and T(dew)T also the hybrid GGA functional MPW1K,[6] especially suited for transition state structures,[7] was tested.

Two different repair mechanisms of Dewar-photolesions are considered for all four Dewar dinucleotides. First, the radical anionic repair (via the doublet-state) subsequent to electron injection by (6-4) photolyase has been investigated (see table SI1). This mechanism is supported by theoretical studies on model systems (the Dewar isomer of 5-Methyl-2-Pyrimidinone and unlinked Dewar dinucleotides)[8] finding that e-injection into the lesion substantially lowers the activation energies ΔE_A for reversion of the Dewar-bicyclus. Experimentally it has been shown,[9] that fully reduced $FADH^-$ is crucial for the repair of the T(dew)C lesion. As second mechanism we calculated the activation energies ΔE_A via the singlet-state (see table SI2).

The activation energies ΔE_A for the radical anionic repair (see table SI1 and Fig.2) is calculated as the difference between the optimized radical-anionic structures, subsequent to electron injection, and the respective transition state of the Dewar-reversion. All stationary points were characterized by normal mode analysis. For the activation energies ΔE_A the lowest energy structure of the dinucleotides was chosen. For a comparison of hydrogen-bond (H-bond) effects additional H-bond conformers were optimized and used for the calculation of reaction barriers in T(dew)C and T(dew)^{m}C (see table SI1, indicated with † and Fig. SI1).

Table SI1: Activation energies ΔE_A of radical-anionic Dewar photolesion repair for the four different substitution patterns in T(dew)C, T(dew)^{m}C, T(dew)U and T(dew)T. All activation energies ΔE_A are given in [eV], the standard basis-set is 6-31G* unless any other basis-set is indicated.

† the radical-anionic Dewar-valence isomers T(dew)C and T(dew)^{m}C can be stabilized in two different H-bond conformers. The different structures are shown in Fig. SI1.

PCM	Functional	T(dew)C	T(dew)^{m}C	T(dew)U	T(dew)T
H_2O (ε=78.4)	M05-2X	0.106 0.144 †	0.181 0.219 †	0.145	0.323
	M06-2X	0.096	0.140	0.102	0.331
	B3LYP	0.068	0.080	0.089	0.146
	MPW1K	0.284	-	-	0.415
	M05-2X (6-31+G*)	0.085	-	-	-
	M05-2X (6-31+G**)	0.096	-	-	-
Dibutylether (ε=3)	M05-2X	0.147	-	-	0.202
	B3LYP	0.051	-	-	0.060
	MPW1K	0.239	-	-	0.270

Table SI2: Activation energies ΔE_A for the Dewar-lesion reversion via the singlet-state. For the four different substitution patterns in T(dew)C, T(dew)^{m}C, T(dew)U and T(dew)T the activation energies ΔE_A are given in [eV], the basis-set is 6-31G*.

PCM	Functional	T(dew)C	T(dew)^{m}C	T(dew)U	T(dew)T
H_2O (ε=78.4)	M05-2X	1.601	1.615	1.595	1.634

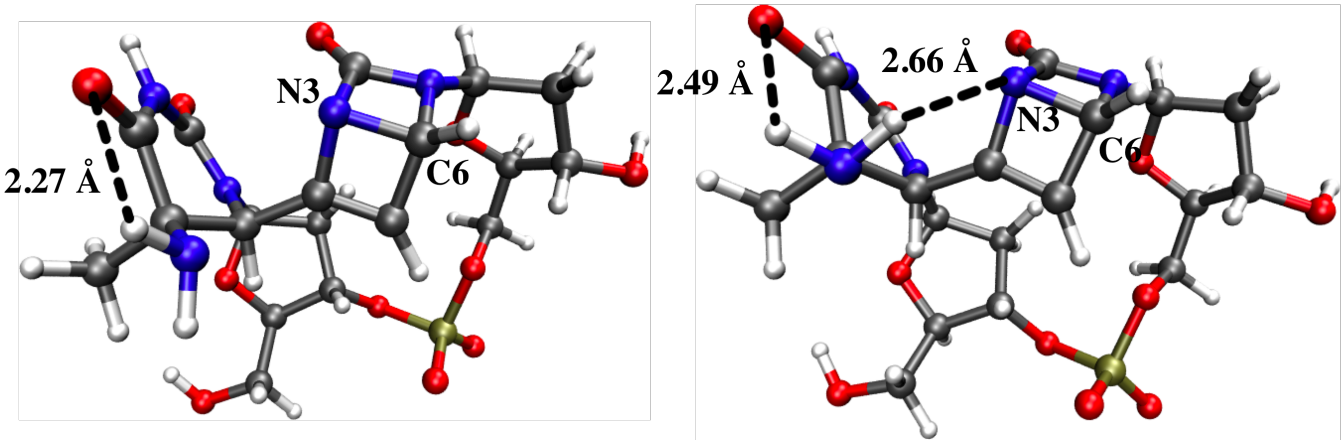

Figure SI1: Optimized geometries of two different H-bond conformers in the radical-anionic Dewar-valence isomer T(dew)C. The structure of the global minimum (right) is stabilized by two H-bonds. Activation energies ΔE_A in table SI1 marked with † correspond to the minimum structure of higher potential energy (left).

The calculated activation energies ΔE_A of the radical-anionic Dewar photolesion repair show the lowest barriers for the T(dew)C lesion and the highest barriers for T(dew)T for all functionals used (Table SI1). The barriers for T(dew)^{m}C lie in between. The B3LYP functional tends to underestimate

the reaction barriers, an effect documented in literature.[10] The results for the M06-2X and M05-2X functionals are nearly identical. Compared to these the hybrid meta-GGA functionals, the MPW1K functional tends to overestimate the reaction barriers, but the ordering in the magnitude of ΔE_A is preserved. The increase of the basis set (6-31G* vs. 6-31+G* vs. 6-31+G**) only slightly effects the reaction barriers ΔE_A (0.106 eV vs. 0.085 eV vs. 0.096 eV). Based on this comparison the activation energies ΔE_A obtained with the M05-2X functional and the 6-31G* basis set are used for the kinetic modeling of the Dewar photolesions repair process catalyzed by (6-4) photolyase (see below).

The calculated activation energies ΔE_A of the neutral Dewar photolesion repair via the singlet-state are substantially increased for all four Dewar-lesions ($\Delta E_A \approx 1.6$ eV, see Table SI2). The increase in ΔE_A allows to exclude the repair mechanism without electron injection and emphasizes the catalytic function of the enzyme.

QM/MM calculations:

To investigate the influence of the surroundig on the activation energies ΔE_A we considered the Dewar-lesion repair in the native environment of the 6-4-photolyase for the T(dew)C and T(dew)T dinucleotides. The recently published crystal structure of the Dewar-substrate bound 6-4-photolyase (pdb code: 2WQ6)[9] serves as starting structure for the QM/MM investigations using the NWchem program package (version 6.0).[11] The position of all crystal waters was preserved.

The protonation states of the amino acids in (6-4) photolyase and DNA fragments were taken as tabulated by the AMBER99 [12] standard parameter files in NWChem. For the $FADH^-$ - cofactor the force field parameters were taken from Ref. [13]. The partial charges of both Dewar-dinucleotides were obtained by fitting the quantum mechanical electrostatic potential with the electrostatic potential (ESP) module of the NWchem program package, the remaining force field parameters were taken from those available in the AMBER99 force field database.[12] To neutralize the charges, 15 Na^+-Ions were added and the system was solvated in a rectangular box of 100 x 100 x 120 Å of SPC/E water,[14] resulting in a total of 118969

atoms. All water molecules and the entire enzyme-DNA substrate complex were initially optimized with the Dewar-lesion dinucleotides represented by ESP charges. The optimization was performed by an alternating optimization of the MM-solvent region and the MM-(6-4) photolyase - DNA complex. In the initial MM-optimization the active site of the (6-4) photolyase and the tightly bound DNA substrate turned out to be stable, a result that has recently been also repoted by Sadeghian *et al*. in an elaborate QM/MM study on the 6-4PP.[15]

The QM/MM calculations are based on a quantum representation of the respective Dewar-dinucleotide (61 QM-atoms in T(dew)C and 63 QM-atoms in T(dew)T, respectively) capped with hydrogen atoms in the Coulomb field of the entire (6-4) photolyase-DNA complex (9642 point charges). The QM/MM calculations are perfomed with the M05-2X functional (basis set: 6-31G*) and start with the initial optimization of the Dewar-lesion in the active site of the enzyme, followed by a second optimization of the radical-anionic form subsequent to electron injection by the (6-4) photolyase. Lesion repair was investigated by a relaxed potential energy scan of Dewar-to-6-4 reversion along the N3-C6 reaction coordinate (Fig. SI1) in the fixed enzyme active site by introducing a harmonic spring as extra potential energy term in the Hamiltonian. The profile of the relaxed potential energy scan served as a starting point for the optimization of the transtion states (TS) of the lesion repair (see Fig. SI2). The activation energies ΔE_A for repair of T(Dew)C and T(Dew)T are defined by the difference in the QM/MM-energy of the localized TS and the relaxed radical anionic Dewar lesions (Table SI3).

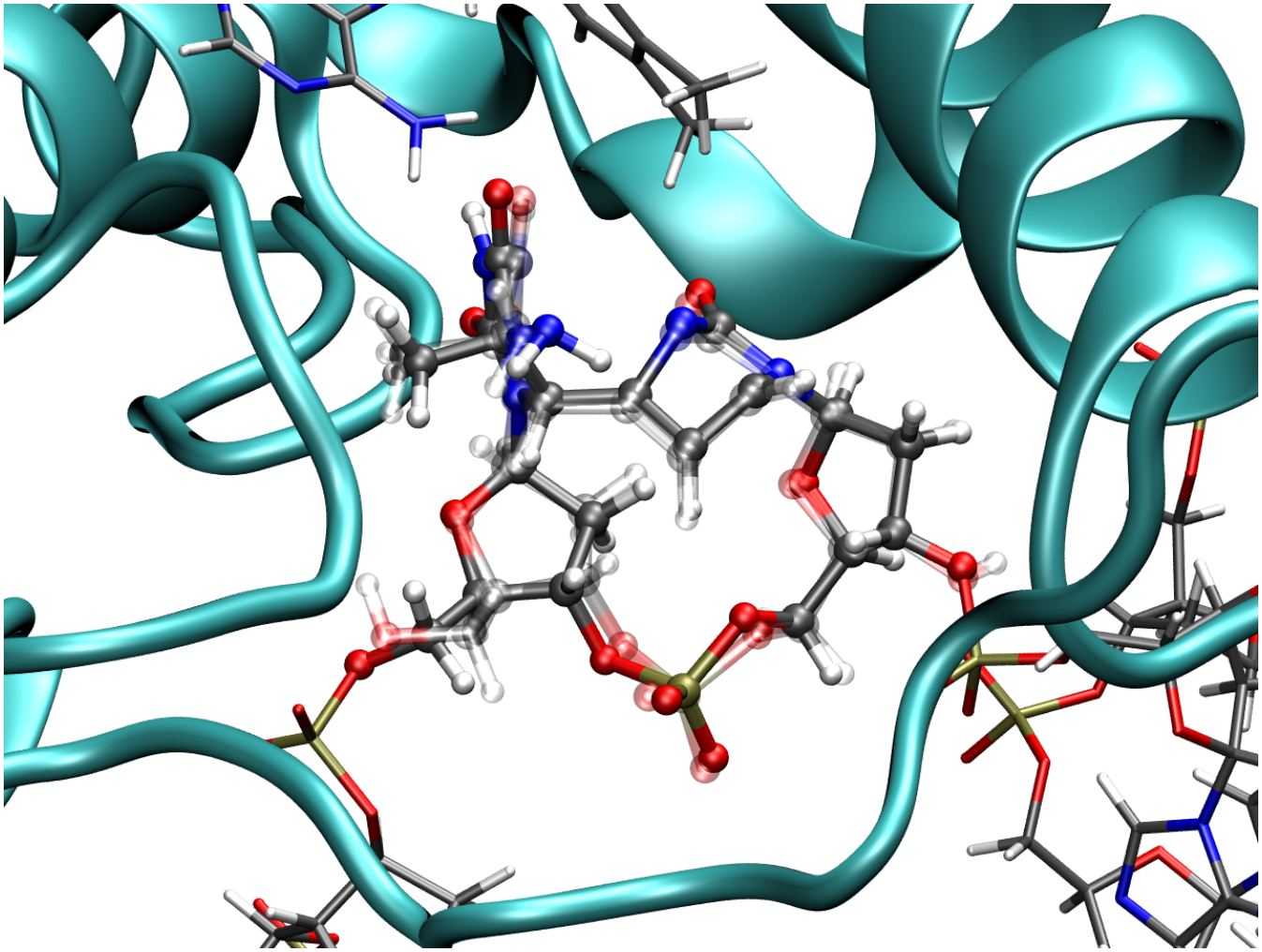

Figure SI2: superimposed structures of the T(Dew)C transition state in the active site of (6-4) photolyase (QM/MM) and in aqueous surrounding (PCM = H2O, transparent). The root-mean-square displacement (RMSD) between the superimposed structures is 0.06 Å for the Dewar part of the molecule, 0.48 Å for both nucleosides and 0.55 Å for the complete dinucleotide.

Table SI3: Activation energies ΔE_A of Dewar photolesion repair for the two different combinations T(dew)C and T(dew)T in the active site of (6-4) photolyase ((6-4) PL) derived from QM/MM calculations. For a comparison the ΔE_A's calculated in aqueous surrounding (see Table SI1) are (H_2O/PCM). All activation energies ΔE_A are given in [eV], functional: M05-2X, basis: 6-31G*.

model	T(dew)C	T(dew)T
(6-4) PL	0.158	0.256
H_2O/PCM	0.106	0.323

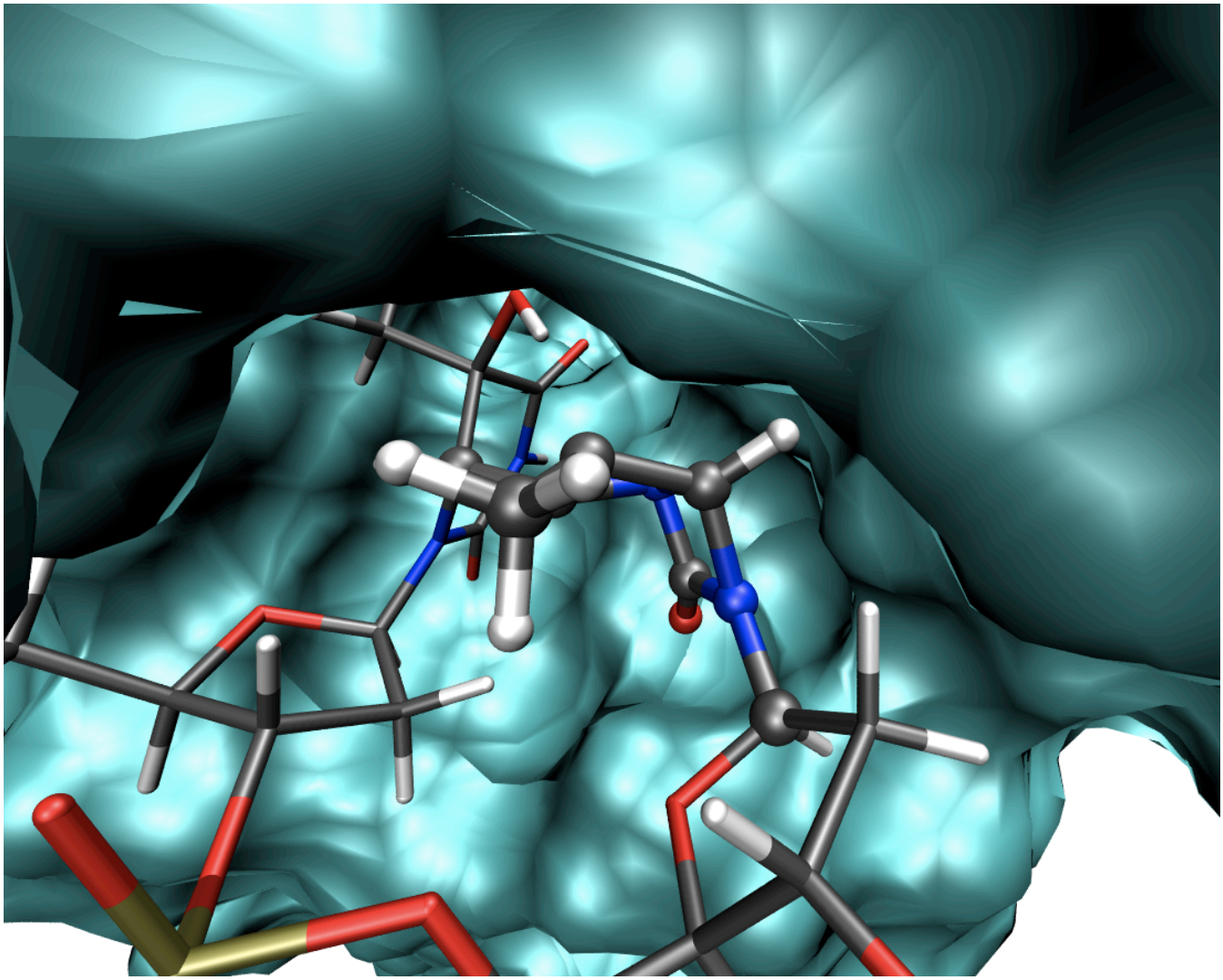

Figure SI3: active site of the (6-4) photolyase bound with a T(Dew)T lesion. The volume of the enzyme is shown in green. The active site is large enough to bind lesions with a Me-group at the C5' position.

Kinetik model for Dewar lesion repair catalyzed by (6-4) photolyase:

To estimate the limits for the Dewar repair we performed kinetic modeling according to the scheme shown in Fig. 3 (a) and Scheme SI1. The model is based on the recent time resolved data for the 6-4PP published by Zhong and Sancar[16] and is extended to the repair of the different Dewar-lesions studied.

We determined the thermally activated rates of lesion repair k_{rep} using classical TST-theory [17]

$$k_{rep} = \nu_{react} * \exp\left(\frac{-\Delta E_A}{k_B T}\right), \qquad \text{(SI 1)}$$

where an unimolecular reaction on a single potential energy surface and a transmission coefficient equal unity have been assumed. For the activation energy ΔE_A the calculated *ab initio* values are taken (Table SI1). The reactive frequency ν_{react} is derived from normal mode analysis and corresponds to the N3-C6 stretch-vibration along the reaction coordinate (992 cm^{-1}).

With the known time constants for $FADH^{-*}$ deactivation k_{deact} (= 1/3 ns^{-1}), the rate of electron injection k_{inj} (= 1/250 ps^{-1}) from $FADH^{-*}$ into the lesion and the rate of charge recombination k_{rec} (= 1/50 ps^{-1}),[16] we can determine the relative quantum yield of Dewar lesion repair by 6-4- photolyase as a function of ΔE_A (see Fig. SI4), by diagonalizing the respective rate matrix. Here we assume that electron injection (k_{inj}) and charge recombination (k_{rec}) for the different Dewar lesions and the (6-4PP investigated in Ref. [16] follow equal kinetics. This assumption is justified by the identical FADH – C=O tunneling distances in all lesions,[9] as the C=O group of the 5,6-dihydrothmidine part is not affected by the substitution pattern investigated in this study.

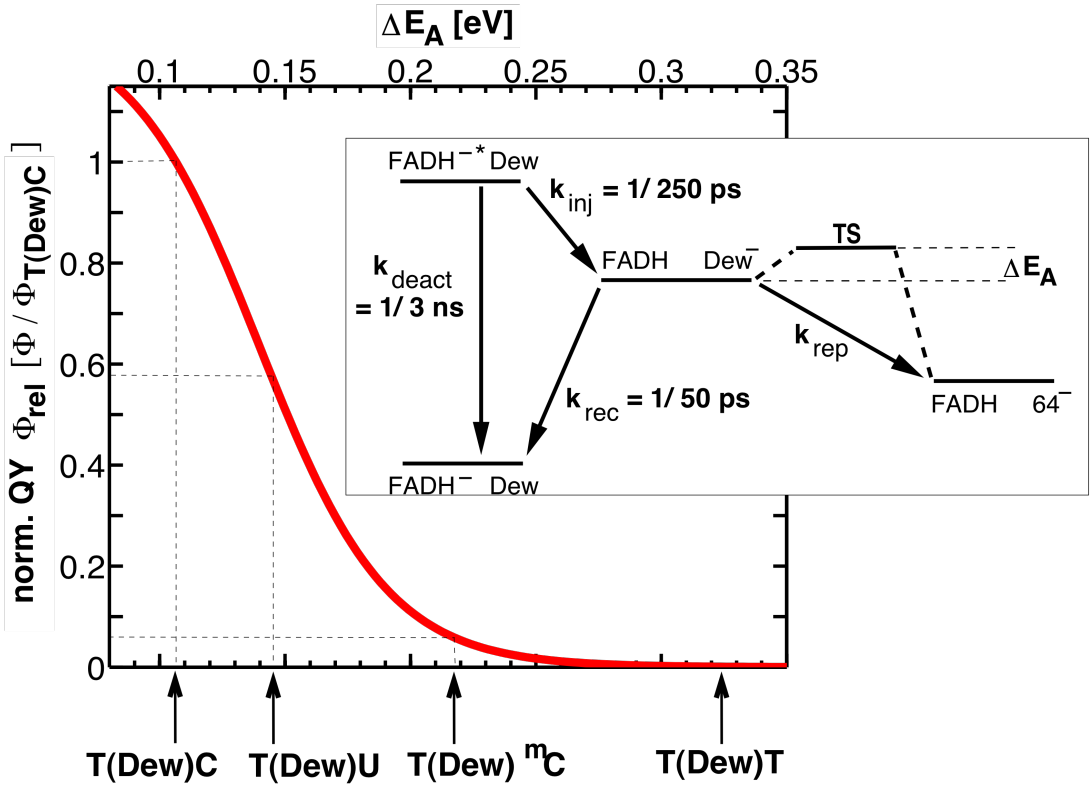

Scheme SI1: Inlay: kinetic model for Dewar lesion repair by 6-4- photolyase; the relative quantum yield Φ_{rel} of Dewar repair as a function of the activation energy ΔE_A are depicted as red line. ΔE_A of the investigated Dewar photolesions (see Table SI1 and Table 1) are indicated with arrows.

For efficient repair of the respective Dewar lesions k_{rep} has to compete directly with the rate of charge recombination k_{rec}. As depicted in Scheme SI1, we set the quantum yield for repair of the T(Dew)C lesion to Φ_{rel} =1. The relative repair quantum yield for the other Dewar lesions are T(Dew)U: Φ_{rel} = 0.57; T(Dew)^{m}C: Φ_{rel} = 0.06; and T(Dew)T: Φ_{rel} = 0 in excellent agreement with the experimentally determined relative quantum yields (see Fig. 1). The catalytic action of (6-4) photolyase relies on the electron injection properties as compared to the isolated dinucleotides no geometric changes are observable at the transition state. Thus the calculated transition state energies and geometries fully explain the experimental observations that Dewar lesion repair by (6-4) photolyase is sensitive to the substitution pattern of the respective lesions, especially at the C5' position.

Experimental Methods:

General

Analytical and preparative HPLC were performed on *Waters* HPLC systems using Nucleodur columns (250 * 4 mm, C18ec, particle size 3 µm or 250 * 10 mm, C18ec, 5 µm) from *Machery-Nagel*. MALDI-TOF mass spectra were recorded on a *Bruker Autoflex II*. The unirradiated oligonucleotides were obtained from *Metabion GmbH* (Martinsried, Germany). The final concentration of the purified oligonucleotides and enzyme concentrations were determined with a *NanoDrop ND-1000* spectrophotometer (*Peqlab*). UV-VIS spectra were recorded on a *JASCO V-650* spectrometer at 25 °C using a 1000 µL quartz cuvette. The irradiation experiments were performed with an UV lamp ((254nm, Vilber Lourmat VL-215C, 2×15 W 254 nm tubes) or (365 nm Black Light, VL-315.BL, 3×15 W 365 nm tubes)) from *ltf Labortechnik GmbH & Co. KG*. HPLC grade solvents were bought from *Fisher Scientific*.

HPLC conditions

Analytical HPLCs were performed on a *Waters* system using 3 µm C_{18}-reversed phase Nucleodur columns from *Machery-Nagel*. Eluting buffers were buffer A (0.1 M TEAA in H_2O) and buffer B (0.1 M TEAA in H_2O/MeCN 20/80). Preparative HPLC was also performed on a *Waters* system using Nucleodur columns (C18ec, 250*10 mm, 5 µm particle size) C_{18}-reversed phase from *Machery-Nagel*. Elution was always monitored at 260 nm and 325 nm.

Mass spectra

MALDI-TOF mass spectra were recorded on a *Bruker Autoflex II* mass spectrometer using 3-hydroxypicolinic acid as matrix substance. The measurement was arranged in the positive polarity mode.

Irradiation experiments, repair assays

Oligonucleotides containing the Dewar isomers were produced and purified using published procedures.[18]

Cloning, protein expression and purification

The (6-4) photolyase from *Drosophila melanogaster* was cloned and purified as described previously.[19]

Table SI4: Sequences of the irradiated oligonucleotides and MALDI-TOF mass spectrometry data, together with the final yield of the 6-4PP containing oligonucleotides.

Number	Sequence (5' → 3')	$[M+H]^+$ (calc.)	$[M+H]^+$ (found)
ODN 1	AGGT(Dew)TGGC	2467	2466
ODN 2	AGGT(Dew)CGGC	2452	2453
ODN 3	AGGT(Dew)UGGC	2453	2452
ODN 4	AGGT(Dew)^{m}CGGC	2466	2466

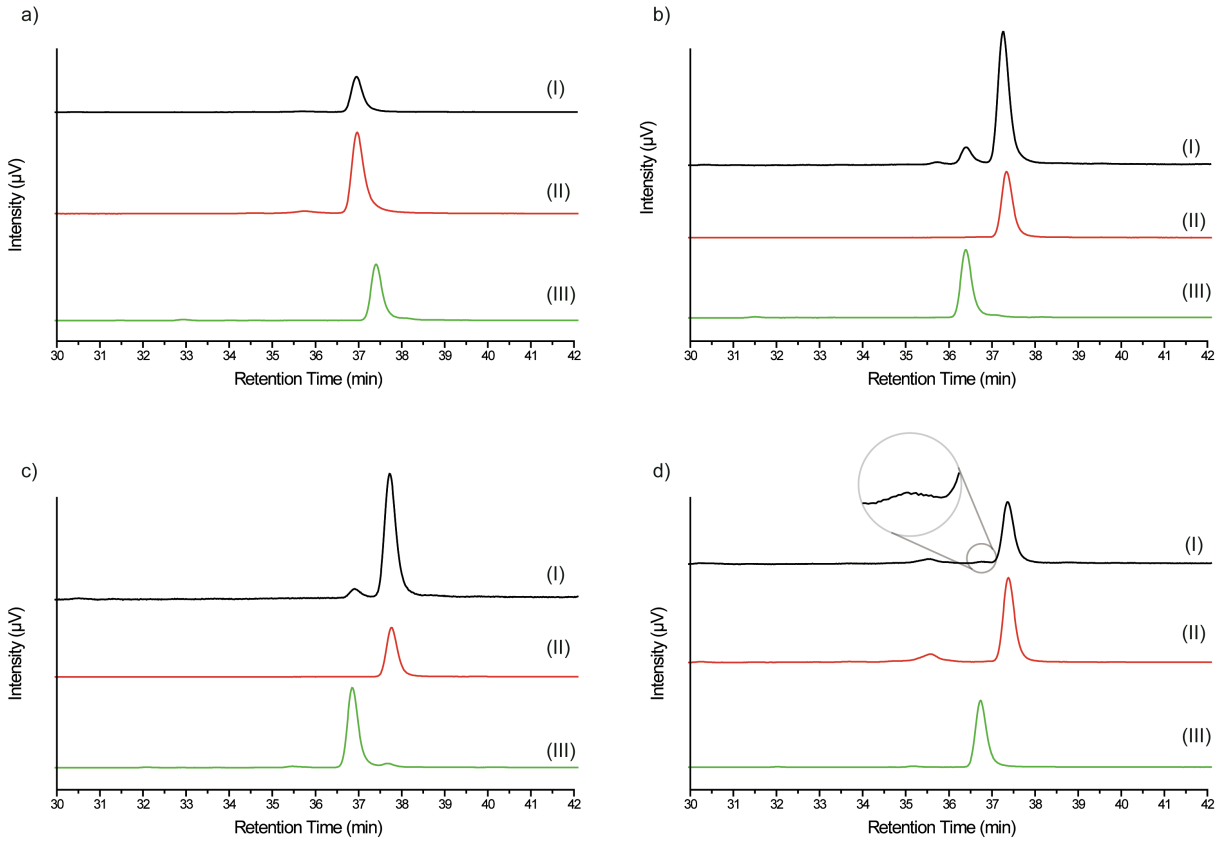

Figure SI4: Analysis of Dewar valence isomer reaction with (6-4) photolyase from D. melanogaster. a) 5'-AGGT(Dew)TGGC-3', b) 5'-AGGT(Dew)CGGC-3', c) 5'-AGGT(Dew)UGGC-3', d) 5'-AGGT(Dew)^{m}CGGC-3'. HPLC chromatogram of the assay containing the corresponding Dewar isomers and the enzyme after 1 h (I). (II) Chromatogram of the corresponding Dewar lesion containing oligonucleotide. (III) Chromatogram of the corresponding undamaged oligonucleotide. The assay and HPLC conditions are described above. The elution was monitored at 260 nm.

REFERENCES

1. Zhao, Y.; Schultz, N. E.; Truhlar, D. G., Exchange-correlation functional with broad accuracy for metallic and nonmetallic compounds, kinetics, and noncovalent interactions. *J. Chem. Phys.* **2005,** *123* (16), 161103.
2. Zhao, Y.; Truhlar, D. G., The M06 suite of density functionals for main group thermochemistry, thermochemical kinetics, noncovalent interactions, excited states, and transition elements: two new functionals and systematic testing of four M06-class functionals and 12 other functionals. *Theor. Chem. Acc.* **2008,** *120*, 215-241.
3. (a) Mennucci, B.; Cancès, E.; Tomasi, J., Evaluation of Solvent Effects in Isotropic and Anisotropic Dielectrics, and in Ionic Solutions with a Unified Integral Equation Method: Theoretical Bases, Computational Implementation and Numerical Applications. *J. Phys. Chem. B* **1997,** *101*, 10506-10517; (b) Tomasi, J.; Mennucci, B.; Cammi, R., Quantum mechanical continuum solvation models. *Chem. Rev.* **2005,** *105* (8), 2999-3093.
4. Gaussian 09, R. A., M. J. Frisch, G. W. Trucks, H. B. Schlegel, G. E. Scuseria, M. A. Robb, J. R. Cheeseman, G. Scalmani, V. Barone, B. Mennucci, G. A. Petersson, H. Nakatsuji, M. Caricato, X. Li, H. P. Hratchian, A. F. Izmaylov, J. Bloino, G. Zheng, J. L. Sonnenberg, M. Hada, M. Ehara, K. Toyota, R. Fukuda, J. Hasegawa, M. Ishida, T. Nakajima, Y. Honda, O. Kitao, H. Nakai, T. Vreven, J. A. Montgomery, Jr., J. E. Peralta, F. Ogliaro, M. Bearpark, J. J. Heyd, E. Brothers, K. N. Kudin, V. N. Staroverov, R. Kobayashi, J. Normand, K. Raghavachari, A. Rendell, J. C. Burant, S. S. Iyengar, J. Tomasi, M. Cossi, N. Rega, J. M. Millam, M. Klene, J. E. Knox, J. B. Cross, V. Bakken, C. Adamo, J. Jaramillo, R. Gomperts, R. E. Stratmann, O. Yazyev, A. J. Austin, R. Cammi, C. Pomelli, J. W. Ochterski, R. L. Martin, K. Morokuma, V. G. Zakrzewski, G. A. Voth, P. Salvador, J. J. Dannenberg, S. Dapprich, A. D. Daniels, Ö. Farkas, J. B. Foresman, J. V. Ortiz, J. Cioslowski, and D. J. Fox, Gaussian, Inc.. Wallingford CT: 2009.
5. Becke, A. D., Density-functional thermochemistry. III. The role of exact exchange. *J. Chem. Phys.* **1993,** *98*, 5648-5652.
6. Lynch, B. J.; Fast, P. L.; Harris, M.; Truhlar, D. G., Adiabatic connection for kinetics. *J. Phys. Chem. A* **2000,** *104* (21), 4811-4815.
7. Lynch, B. J.; Truhlar, D. G., How well can hybrid density functional methods predict transition state geometries and barrier heights? *J. Phys. Chem. A* **2001,** *105* (13), 2936-2941.
8. (a) Wang, Y. S.; Gaspar, P. P.; Taylor, J. S., Quantum chemical study of the electron-transfer-catalyzed splitting of oxetane and azetidine intermediates proposed in the photoenzymatic repair of (6-4) photoproducts of DNA. *J. Am. Chem. Soc.* **2000,** *122* (23), 5510-5519; (b) Ai, Y. J.; Liao, R. Z.; Chen, S. F.; Luo, Y.; Fang, W. H., Theoretical studies on photoisomerizations of (6-4) and Dewar photolesions in DNA. *J. Phys. Chem. B* **2010,** *114* (44), 14096-14102.
9. Glas, A. F.; Kaya, E.; Schneider, S.; Heil, K.; Fazio, D.; Maul, M. J.; Carell, T., DNA (6-4) photolyases reduce Dewar isomers for isomerization into (6-4) lesions. *Journal of the American Chemical Society* **2010,** *132*, 3254-3255.
10. Lingwood, M.; Hammond, J. R.; Hrovat, D. A.; Mayer, J. M.; Borden, W. T., MPW1K performs much better than B3LYP in DFT calculations on reactions that proceed by proton-coupled electron transfer (PCET). *J. Chem. Theory Comput.* **2006,** *2* (3), 740-745.
11. Valiev, M.; Bylaska, E. J.; Govind, N.; Kowalski, K.; Straatsma, T. P.; Dam, H. J. J. v.; Wang, D.; Nieplocha, J.; Apra, E.; Windus, T. L.; Jong, W. A. d., NWChem: a comprehensive and scalable open-source solution for large scale molecular simulations. *Comput. Phys. Commun.* **2010,** *181*, 1477
12. (a) Wang, J.; Cieplak, P.; Kollman, P. A., How Well Does a Restrained Electrostatic Potential (RESP) Model Perform in Calculating Conformational Energies of Organic and Biological Molecules? *J. Comput. Chem.* **2000,** *121*, 1049–1074; (b) Cornell, W. D.; Cieplak, P.; Bayly, C. I.; Gould, I. R.; Kenneth, l.; M. Merz, J.; Ferguson, D. M.; Spellmeyer, D. C.; Thomas Fox;

Caldwell, J. W.; Kollman, P. A., A Second Generation Force Field for the Simulation of Proteins, Nucleic Acids, and Organic Molecules. *J. Am. Chem. Soc.* **1995,** *117*, 5179-5197.

13. Antony, J.; Medvedev, D. M.; Stuchebrukhov, A. A., Theoretical Study of Electron Transfer between the Photolyase Catalytic Cofactor FADH- and DNA Thymine Dimer. *J. Am. Chem. Soc.* **2000,** *122*, 1057-1065.
14. Berendsen, H. J. C.; Grigera, J. R.; Straatsma, T. P., THE MISSING TERM IN EFFECTIVE PAIR POTENTIALS. *J. Phys. Chem.* **1987,** *91* (24), 6269-6271.
15. Sadeghian, K.; Bocola, M.; Merz, T.; Schutz, M., Theoretical study on the repair mechanism of the (6-4) photolesion by the (6-4) photolyase. *J. Am. Chem. Soc.* **2010,** *132* (45), 16285-16295.
16. Li, J.; Liu, Z.; Tan, C.; Guo, X.; Wang, L.; Sancar, A.; Zhong, D., Dynamics and mechanism of repair of ultraviolet-induced (6-4) photoproduct by photolyase. *Nature* **2010,** *466* (7308), 887-890.
17. (a) Garcia-Viloca, M.; Gao, J.; Karplus, M.; Truhlar, D. G., How enzymes work: Analysis by modern rate theory and computer simulations. *Science* **2004,** *303* (5655), 186-195; (b) de la Lande, A.; Rezac, J.; Levy, B.; Sanders, B. C.; Salahub, D. R., Transmission Coefficients for Chemical Reactions with Multiple States: Role of Quantum Decoherence. *J. Am. Chem. Soc.* **2011,** *133* (11), 3883-3894; (c) Jortner, J., TEMPERATURE-DEPENDENT ACTIVATION-ENERGY FOR ELECTRON-TRANSFER BETWEEN BIOLOGICAL MOLECULES. *J. Chem. Phys.* **1976,** *64* (12), 4860-4867.
18. Glas, A. F.; Schneider, S.; Maul, M. J.; Hennecke, U.; Carell, T., Crystal structure of the T(6-4)C lesion in complex with a (6-4) DNA photolyase and repair of UV-induced (6-4) and Dewar photolesions. *Chemistry* **2009,** *15* (40), 10387-10396.
19. Maul, M. J.; Barends, T. R.; Glas, A. F.; Cryle, M. J.; Domratcheva, T.; Schneider, S.; Schlichting, I.; Carell, T., Crystal structure and mechanism of a DNA (6-4) photolyase. *Angew. Chem., Int. Ed. Engl.* **2008,** *47* (52), 10076-10080.